EMPIRICAL MIXING MODEL FOR THE ELECTRO-MAGNETIC MODELLING OF ON-CHIP INTERCON-NECTS

S. M. Holik[*], J. M. Arnold, and T. D. Drysdale

Electronics Design Centre, Division of Electronics and Nanoscale Engineering, School of Engineering, University of Glasgow
Rankine Bld., Oakfield Avenue, Glasgow G12 8LT, United Kingdom

Abstract—We present an empirical mixing model for rectangular cuboid metal inclusions in a host dielectric, suitable for replacing the detailed structure of a layer of on-chip interconnects with a homogeneous dielectric slab. Such an approximation is required to facilitate the accurate and efficient package-level electromagnetic modelling of complicated miniaturised systems, such as System-in-Package. Without such an approach, the direct inclusion of large areas of on-chip interconnect structures often results in intractable computation times. Our model allows us to predict the reflection (transmission) coefficient of impinging plane waves to within 3.5% (0.2%) error for incident angles up to 30° off-normal, aspect ratios 0.6–3, metal fill factors 0.3–0.6, and host dielectric constants 1–11.7, over the frequency range 1–10 GHz.

1. INTRODUCTION

It is computationally demanding to directly simulate large areas of on-chip interconnects with full vector electromagnetic solver tools, due to the amount of memory required to hold the detailed mesh, and numerical penalties associated with small mesh cell sizes relative to the wavelengths of the signals being modelled [1]. Though such large simulations can be done on isolated structures [2] the high resolution and computational demand is not desirable when they are part of a large scale simulation [3–5]. The ongoing miniaturisation of large, complex systems into single packages, such as System-in-Package, is expected to lead to a requirement for the on-chip interconnects of

each of the constituent chips to be accounted for in package-level electromagnetic simulations. From a package-level point of view, the on-chip interconnects can be seen as a mixture of metal inclusions located in a host dielectric. In other applications, it has been shown that the macroscopic properties of dielectric-only mixtures can be represented by a homogeneous dielectric with an effective permittivity that is determined using an empirical mixing model [6]. Metal-dielectric mixtures have been less thoroughly explored, with work limited to treating spherical or ellipsoidal metal inclusions [7, 8]. In this paper, we extend the approach to cope with rectangular cuboid metal inclusions representative of on-chip interconnect structures. We retain the use of a single fitting parameter, which is calculated for a wide range of aspect ratios, dielectric host materials, metal fill factors and signal frequencies that are likely to be of interest to System-in-Package designers.

2. METHODOLOGY

Interconnects often form regular gratings (e.g., bus structures), hence an infinite metallic grating in a homogeneous dielectric host, as shown in Fig. 1, represents a straightforward but broadly applicable model.

We considered a wide parameter space for the dimensions, as follows. Design rules often specify interconnect pattern density can be in the range of 20%–80% metal fill [9], but often the maximum pattern density in actual metal layers does not exceed 60% [10]. Thus we consider metal fill factors f in the range 0.2–0.6. While metal layer height is fixed for any given layer in any given process, track width is less restricted. Aspect ratios (x_{AR}) are continuing to increase as technology develops [11], hence we studied structures with $0.6 \leq x_{AR} \leq 3$. Due to the growing use of low-k dielectrics we considered host materials with permittivity ϵ_e in the range $1 \leq \epsilon_e \leq 11.7$. The interconnect pitch Λ is often measured in micrometres or nanometres,
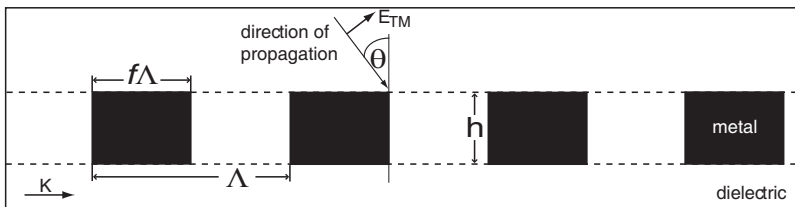

Figure 1. Diagram of studied 2-D grating structure with dashed line indicating the boundaries of the homogenised equivalent.

whereas the wavelength λ of the clock signal is typically measured in centimetres. Thus, we can expect to successfully apply an appropriate effective medium approximation because the condition $\Lambda \ll \lambda/4$ is met [12]. Here, we fix $\Lambda = 100 \, \mu m$ for the sake of clarity in illustrating our method. While we include the effect of the interlevel dielectric, we omit the bulk substrate and all but the top layer of interconnects from the homogenisation process in order to reduce the complexity of this initial study. We use a modified Maxwell-Garnett mixing rule

$$\epsilon_{\text{eff}} = \epsilon_e + \Psi f \epsilon_e \frac{\epsilon_i - \epsilon_e}{\epsilon_i + 2\epsilon_e - f(\epsilon_i - \epsilon_e)}, \tag{1}$$

where ϵ_i and ϵ_e are the dielectric functions of the inclusion and host material respectively (here, a metal and a dielectric), Ψ is a constant relating the fields inside and outside the inclusions (typically $\Psi = 3$ for spherical inclusions), f is the filling factor or ratio of the volume of the inclusion to the total size of the unit cell [13]. In earlier work we presented a limited example of our approach for a fixed value of Ψ applicable to a single structure [14, 15]. Further we have significantly expanded our approach by developing a compact equation to calculate the appropriate value of Ψ for a broad range of parameters [16] and here we provide more detailed analysis of the distribution of Ψ values.

3. RESULTS

Rigorous coupled wave analysis (RCWA) [17] was performed for the TM polarization with the electric field vector $\mathbf{E}_{TM}$ coplanar with the grating vector $\mathbf{K}$ as shown in Fig. 1. The metal inclusions were assumed to have a frequency dependent dielectric function $\epsilon_i(\omega)$ that is represented by a Drude model [18]

$$\epsilon_i(\omega) = 1 - \frac{\omega_p^2}{\omega(\omega + j\gamma)}, \tag{2}$$

where ω is the frequency of interest, ω_p is the plasma frequency and γ is a damping term representing energy dissipation. Despite wide spread use of copper interconnects for the intermediate levels of the interconnect stack, aluminum is often used for the global wiring with which we are concerned, and has $\omega_p = 15 \, eV$ and $\gamma = 0.1 \, eV$. Note that the energy is related to the free space wavelength λ_0 by $\omega = 1.24 \times 10^{-6} (\lambda_0)^{-1}$. This model was used in both the analytical and numerical calculations. The structure was illuminated by a plane wave with incident angle $-90° < \theta < 90°$ and free-space wavelengths $\lambda = 30 \, cm$, $\lambda = 10 \, cm$, $\lambda = 6 \, cm$, and $\lambda = 3 \, cm$. In results not shown here, we studied the effect of adjusting the height h of the homogenised

Table 1. Coefficients α_{mn} and β_{mn}, where $m, n = \{1, 2\}$, for Ψ calculation.

α_{11}	-0.0054	β_{11}	0.0191	γ_{11}	-0.0370	δ_{11}	0.0026
α_{12}	3.0965	β_{12}	-6.3175	γ_{12}	-1.0792	δ_{12}	-0.0558
α_{21}	0.0188	β_{21}	-0.0086	γ_{21}	0.0231	δ_{21}	-0.0015
α_{22}	3.1421	β_{22}	-1.1014	γ_{22}	2.5738	δ_{22}	-0.0513

layer, but did not find any advantage in doing so. Hence, we kept the height of homogeneous equivalent layer the same as the grating. The reflection coefficient for the homogenised structure was calculated using an analytical formula defined for a stratified medium comprising a stack of thin homogeneous films [19].

It is not necessary to make Ψ dependent on the host dielectric as this is already accounted for explicitly in Eq. (1). We verified this by numerical experiment. The scaling factor Ψ was observed to have an exponential dependence on aspect ratio, as illustrated in Fig. 2, therefore we have chosen the general form of our empirical model to be the sum of two exponentials:

$$\Psi(x_{AR}) = \alpha \cdot e^{\beta \cdot x_{AR}} + \gamma \cdot e^{\delta \cdot x_{AR}} \qquad (3)$$

where the coefficients α, β, γ, δ are determined by linear regression from data obtained from nearly 7000 simulations spanning a four dimensional parameter space. The coefficients are represented as a linear function of metal fill factor by

$$k(f) = k_1 \cdot f + k_2, \quad k = \{\alpha, \beta, \gamma, \delta\} \qquad (4)$$

where k_1, k_2 are well approximated by

$$k_1(\nu) = k_{11} \cdot \nu + k_{12}, \qquad (5)$$
$$k_2(\nu) = k_{21} \cdot \nu + k_{22}, \quad k = \{\alpha, \beta, \gamma, \delta\} \qquad (6)$$

where ν is the frequency (in units of GHz), and factors k_{11}, k_{12}, k_{21}, k_{22} are presented in Table 1.

The model can be applied by choosing values of the four parameters within the specified range of validity and substituting them into equations Eqs. (3)–(6). Since the electromagnetic performance of the interconnect grating structure is frequency dependent, in order to implement the equivalent parameters into a Finite Difference Time Domain (FDTD) model with broadband excitation, the ability to define frequency dependent materials, such as [20, 21] is required.

We assessed the fit of the model using a nonlinear least square method. Fig. 2 illustrates the good agreement between Ψ obtained
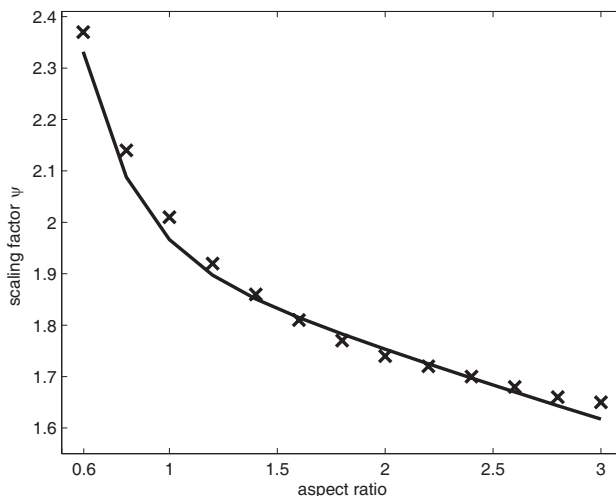
Figure 2. Plot of the scaling factor Ψ obtained for an example grating structure. The fitted values (crosses) show good agreement with approximated data (lines). Grating parameters: $f = 0.5$, $\Lambda = 100\,\mu\text{m}$, $\nu = 5\,\text{GHz}$, $\epsilon_e = 6.25$, $0.6 \leq x_{AR} \leq 3$.

from a 'brute force' fitting algorithm and that from our double exponential approximation for an example grating structure. The grating has $f = 0.5$, and the illumination frequency is $5\,\text{GHz}$. The error in the scaling factor Ψ that is predicted by the least squares method for all background dielectrics, all metal fill factors f, and all frequencies ν as a function of aspect ratio, has an error of 0%–2.5% compared to the values obtained from the 'brute force' fitting algorithm.

In Fig. 3, we plot the reflection coefficient obtained using RCWA and our homogenised model for a sample of 39 different structures. For frequencies in the range $1\,\text{GHz} \leq \nu \leq 10\,\text{GHz}$ the error between RCWA results for the detailed structure and those obtained for the homogenised structure is less than 3.5% for reflection coefficient and 0.2% for the transmission coefficient (not shown here) when $0.3 \leq f \leq 0.6$ and $\theta \leq \pm 30°$. The frequency dependent behavior of the calculated error in reflection and transmission coefficients between grating and homogenised layer with ϵ_{eff} calculated from given formulation for an exemplar structure is shown in Fig. 4. In most of the studied structures with aspect ratio from the middle of the considered range the error in reflection coefficient estimation is less than 1% and it tends to increase and reach the maximum value for an aspect ratio bounding the considered set. This tendency in error distribution
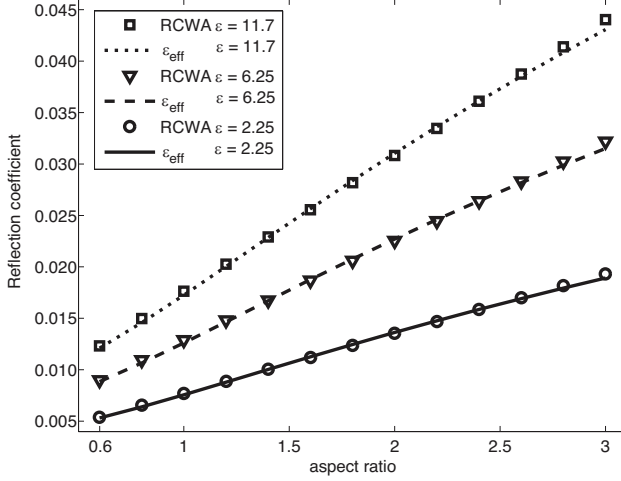
Figure 3. Plot of the reflection coefficient obtained from a subset of the gratings studied, as a function of aspect ratio and host permittivity. Results from the homogenised model are drawn as lines, while those from detailed structure simulated with RCWA are plotted as markers. Fixed parameters: $f = 0.5$, $\nu = 5\,\mathrm{GHz}$.
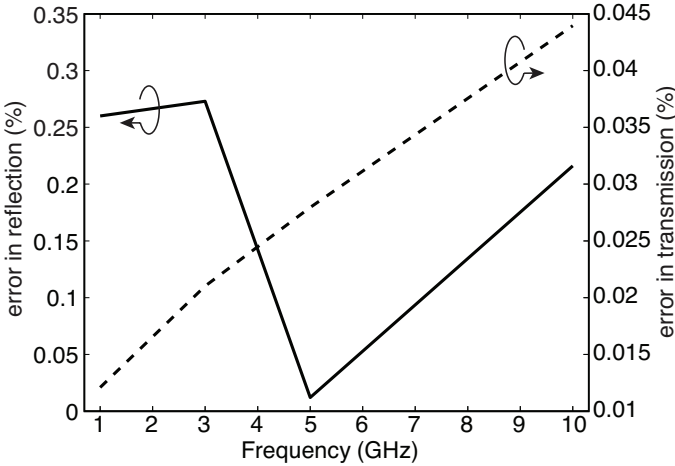

Figure 4. Plot of the frequency dependent error in reflection and transmission coefficients between grating and homogenised layer. The arrows point in the direction of the axis to which the curves belong. Fixed parameters: $f = 0.5$, $x_{AR} = 2$, $\epsilon = 6.25$.

is expected and is related to the curve fitting procedure applied in order to analytically interpret the changes of each variable in the four dimensional parameter space.

When we apply our method, without modification, to interconnects with a trapezoidal cross section, sometimes found in fabricated structures, the error remains below 5% for sidewalls with angles of up to 5° and incident angle up to 30°. Beyond incident angles of ±30°, the error rises, reaching 10% at ±40° and worsening as Brewster's angle is approached. Nonetheless Brewster's angle is predicted to within 5° in the cases we studied, although qualitative agreement beyond Brewster's angle is poor. This arises due to the increased importance of resonant phenomena that cannot be accounted for in a homogenised model [22–24]. Hence our approach offers attractive performance savings over a fully detailed mesh in those cases where incident waves are within ±30° of the normal, such for a Systen-in-Package subject to interference from a distant source.

The computational time gain achieved by using this approach is within 8–25% depending on the geometrical parameters of the grating structure. The higher time gain is obtained for structures with lower metal fill factors and high aspect ratio.

4. CONCLUSION

We report an empirical model for the homogenisation of a single layer of on-chip interconnects that is intended to facilitate their inclusion in package-level electromagnetic simulations. The model is applicable to a wide range of interconnect dimensions (metal fill 20–60%, aspect ratio 0.6–3 and host permittivity 1–11.7) and is accurate to better than 3.5% (0.2%) error for reflection (transmission) when illuminated by plane waves with frequency 1–10 GHz, incident at up to 30° off the normal. Our approach allows the behaviour of on-chip interconnects to be accurately captured in full vector electromagnetic simulations without incurring the significant computational penalties associated with a finely detailed mesh, for a range of incident angles. We expect further developments to include extending the model to cope with multiple interconnect layers, now that the feasibility of the approach has been established.

REFERENCES

1. Stefanski, T. M. and T. D. Drysdale, "Parallel implementation of the ADI-FDTD method," *Microwave Opt. Technol. Lett.*, Vol. 51, No. 5, 1298–1304, 2009.

2. Choi, J., M. Swaminathan, B. Beker, and R. Master, "Modeling of realistic on-chip power grid using FDTD method," *Proc. IEEE Int. Sym. Electromagnetic Compatibility*, Vol. 1, 238–243, 2002.

3. Fontanelly, A., "System-in-Package technology: Opportunities and challenges," *Proc. IEEE 9th International Symposium on Quality Electronic Design (ISQED'08)*, 589–593, 2008.

4. Sham, M. L., Y. C. Chen, J. R. Leung, and T. Chung, "Challenges and opportunities in system-in-package business," *Proc. IEEE 7th International Conference on Electronics Packaging Technology (ICEPT'06)*, 1–5, 2006.

5. Trigas, C., "Design challenges for system-in-package vs system-on-chip," *Proc. IEEE Custom Integrated Circuit Conference (CICC'03)*, 663–666, 2003.

6. Karkkainen, K., A. Sihvola, and K. Nikoskinen, "Analysis of three-dimensional dielectric mixture with finite difference method," *IEEE Trans. Geosci. Remote Sensing*, Vol. 39, No. 5, 1013–1018, 2001.

7. Chylek, P. and V. Srivastava, "Effective dielectric constant of a metal-dielectric composite," *Phys. Rev. B*, Vol. 30, No. 2, 1008–1009, 1984.

8. Sihvola, A., *Electromagnetic Mixing Formulas and Applications*, IEE Publishing, London, UK, 1999.

9. Lakshminarayann, S., P. J. Wright, and J. Pallinti, "Design rule methodology to improve the manufacturability of the copper CMP process," *Proc. IEEE International Interconnect Technology Conference (IITC'02)*, 99–102, 2002.

10. Zarkesh-Ha, P., S. Lakshminarayann, K. Doniger, W. Loch, and P. J. Wright, "Impact of interconnect pattern density information on a 90 nm technology ASIC design flow," *Proc. IEEE 4th International Symposium on Quality Electronic Design (ISQED'03)*, 405–409, 2003.

11. International Technology Roadmap for Semiconductors, Interconnect, Edition 2007, http://www.itrs.net/.

12. Rytov, S. M., "Electromagnetic properties of a finely stratified medium," *Sov. Phys. JETP*, Vol. 2, 466–475, 1956.

13. Maxwell-Garnett, J. C., "Colours in metal glasses and in metallic films," *Phil. Trans. R. Soc. London*, Vol. 203, 385–420, 1904.

14. Holik, S. M. and T. D. Drysdale, "Effective medium approximation for electromagnetic compatibility analysis of integrated circuits," *Proc. 2nd International Congress on Advanced Electromagnetic Materials in Microwaves and Optics*, 413–415, 2008.

15. Holik, S. M. and T. D. Drysdale, "Simplified model of a layer of interconnects under a spiral inductor," *Journal of Electromagnetic Analysis and Applications*, Vol. 3, No. 6, 187–190, 2011.

16. Holik, S. M. and T. D. Drysdale, "Simplified model for on-chip interconnects in electromagnetic modelling of system-in-package," *Proc. 12th International Conference on Electromagnetics in Advanced Applications*, 541–544, 2010.

17. GSolver5.1, Grating Solver Development Company Co., http://www.gsolver.com/.

18. Pendry, J. B., A. J. Holden, W. J. Stewart, and I. Youngs, "Extremely low frequency plasmons in metallic masostructures," *Phys. Rev. Lett.*, Vol. 76, No. 25, 4773–4776, 1996.

19. Born, M. and E. Wolf, *Principles of Optics: Electromagnetic Theory of Propagation, Interference and Diffraction of Light*, 7th Edition, Cambridge University Press, Cambridge, UK, 1999.

20. Rouf, H. K., F. Costen, S. G. Garcia, and S. Fujino, "On the solution of 3-D frequency dependent Crank-Nicolson FDTD scheme," *Journal of Electromagnetic Waves and Applications*, Vol. 23, No. 16, 2163–2175, 2009.

21. Sullivan, D. M., "Frequency-dependent FDTD methods using Z-transform," *IEEE Trans. Antennas Propagat.*, Vol. 40, No. 10, 1223–1230, 1992.

22. Collin, S., F. Pardo, R. Teissier, and J. L. Pelouard, "Horizontal and vertical surface resonances in transmission metallic gratings," *J. Opt. A: Pure Appl. Opt.*, Vol. 4, 154–160, 2002.

23. Pilozzi, L., A. D'Andrea, and H. Fenniche, "Mirror effect at the Brewster angle in semiconductor rectangular gratings," *Phys. Rev. B*, Vol. 64, 235319-1–8, 2001.

24. Barbara, A., P. Quemerais, E. Bustarret, T. Lopez-Rios, and T. Fournier, "Electromagnetic resonances of sub-wavelength rectangular metallic gratings," *Eur. Phys. J. D*, Vol. 23, 143–154, 2003.